



# Finite Element Convergence Study of the Asymmetric Friction Connection (AFC) in the Optimised Sliding Hinge Joint (OSHJ)

*F. Alizadeh & S. Ramhormozian*

Department of Built Environment Engineering, Auckland University of Technology, Auckland.

*G.C. Clifton*

Department of Civil and Environmental Engineering, University of Auckland, Auckland.

## **ABSTRACT**

The Optimised Sliding Hinge Joint (OSHJ) is a cost-effective, low damage seismic resisting beam-column connection developed for Moment Resisting Steel Framed (MRSF) buildings. The OSHJ is the optimised version of the traditional Sliding Hinge Joint. The Asymmetric Friction Connections (AFCs) with partially deflected Belleville Springs (BeSs), named as Optimised Asymmetric Friction Connections (OAFCS) in this paper, are the OSHJ's friction sliding energy dissipating components, which also act as fuses to limit the seismic induced internal actions in the beams and columns. The OAFCS may be installed at the beam bottom flange and web bottom bolts level in the OSHJ. The OAFCS bolts are tightened in the elastic range and remain effectively elastic during seismic induced sliding under severe earthquake demands, retaining most of their installed bolt tension after significant sliding.

This paper provides a brief background on the OSHJ developments, followed by presenting the Finite Element Model (FEM) of the OAFCS using ABAQUS software, including explanation of the FEM's geometrical, material, and boundary condition characteristics. Finally, a convergence (aka sensitivity) study is undertaken, and the optimum mesh size and geometry as well as element type are identified, to be used in the ongoing extensive finite element analysis of these systems.

## **1 INTRODUCTION**

### **1.1 Background**

During a major earthquake (ultimate limit state (ULS) and larger earthquakes) a large amount of energy is imposed on the building due to the building's dynamic response to the input ground excitation. The

mechanism based on which this energy is dissipated within the structure is a key parameter in determining the level of damage. While it is not feasible to design and construct structures to be completely damage resistant under all possible earthquakes, it is readily possible to improve the conventional design and construction approaches to decrease the likelihood and degree of structural damage under major earthquakes and to significantly raise the structural damage threshold.

The building codes recognize that, for most of the buildings, it is economically not feasible to accommodate the energy imposed on the structures within the elastic capacity of the structural materials. Moreover, doing so may result in stiffer and stronger structures for which the dynamic response to particular ground excitations may be increased, causing greater non-structural and contents damage. A key criterion stipulated in current building codes is to satisfy the life safety mandate. However, this means that during an event more severe than the design level event, damage is expected to occur in the structural elements of a well-designed and well-detailed building, which may require repair or even, in many cases, demolition of the building. This will impose significant cost and disruption to the affected communities. Low-damage design and construction has been being developed to address this critical issue.

## 1.2 The low-damage design philosophy

In the seismic design of structures, the ductility concept allows structural designers to undertake a cost-effective design by incorporating post-elastic capacity of the structure. This means the energy is allowed to be dissipated through inelastic deformations of the structural members. However, this is associated with permanent damage. The repair of the damage may be significantly costly and/or not practical [1]. To avoid these undesirable economic effects of earthquakes, following recent several damaging events, the global tendency has been moving towards the development and implementation of low damage seismic resisting systems.

The initial key motivation for the low damage design philosophy developments was the experience in the 1994 Northridge [2] and the 1995 Kobe [3] earthquakes. Significant unexpected damages to the welded connections of multi-story, moment-resisting steel-framed buildings were observed in these events [4].

The low damage design philosophy aims, in addition to satisfying the well-accepted “life safety” mandate, to minimize the economic losses due to post-earthquake damage repair as well as downtime. The importance of this has again been illustrated in further major earthquakes such as the 2010/2011 Canterbury earthquake series, the 2010 Maule earthquake, and the 2016 Kaikoura earthquake [5]. These recent earthquakes have clearly demonstrated that conventional construction, even in technologically advanced countries with well-designed and detailed structures, is not immune to destruction [5, 6].

### 1.2.1 The Sliding Hinge Joint

An example of a low-damage system developed for seismic moment-resisting steel frames (MRFs), one of the most commonly used lateral force resisting systems, is the Sliding Hinge Joint connection (SHJ) with Asymmetric Friction Connections (AFCs) as shown in Figure 1. The AFCs are energy dissipating components of the SHJ.

The SHJ, proposed by Clifton [7] and shown in figure 1, adopted the concept of pinning the beam to the column at the top flange, utilizing the AFC at the bottom flange and bottom web level.

The AFC in the SHJ as shown in the figure 2, consists of five plies, including the beam bottom flange, bottom flange plate (cleat), cap plate, and two shims at both sides of the cleat, all clamped by the pre-

tensioned high strength friction grip (HSFG) structural bolts. The AFC has two main sliding surfaces on both sides of the cleat.

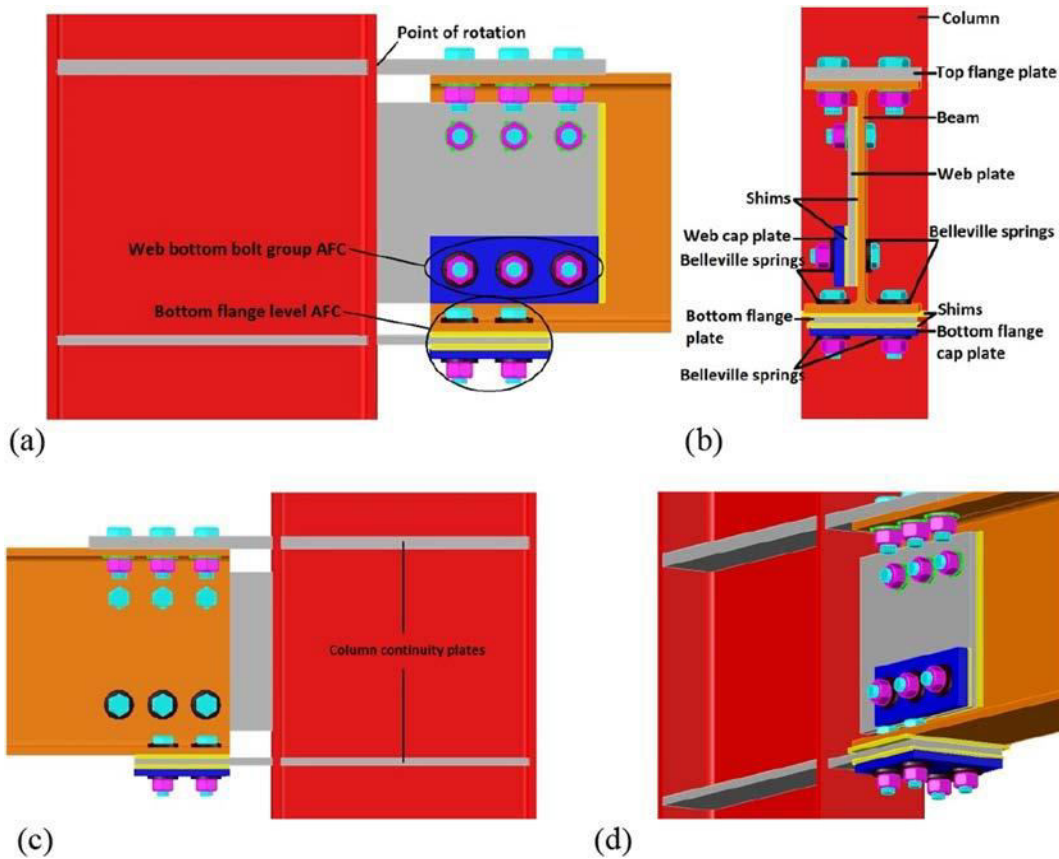


Figure 1: The sliding hinge joint (SHJ) views (a) front (b) beam cross sectional, (c) back, and (d) 3D [6]

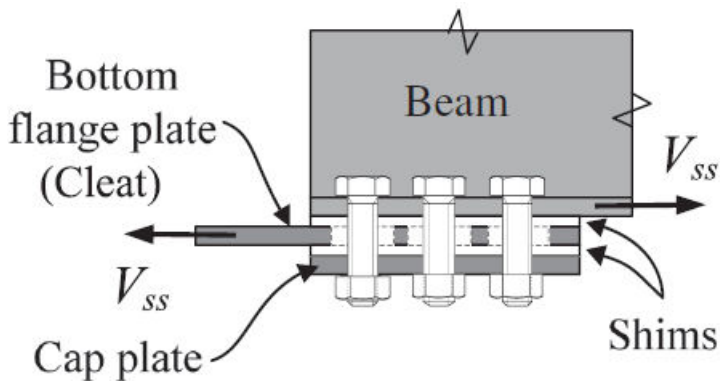


Figure 2: The AFC at the bottom flange level [8]

### 1.2.2 The Optimised Sliding Hinge Joint

In 2017 Ramhormozian et al. [5, 6] showed that using partially deflected Belleville Springs (BeSs) with sufficient axial deformation to reach the installed bolt tension in the elastic range, being installed at both head and nut sides of the AFC bolts, would reduce the post-sliding clamping force loss, improve the self-centering capability, increase the system coefficient of friction, reduce the additional imposed tension on the AFC bolts during stable sliding due to prying actions and/or moment, shear, and axial force (MVP) interactions, and reduce the severity of the sliding surfaces' wearing. BeSs, as shown in figure 3, are

truncated conical washer-type elements of very high strength steel that compress elastically, if they are pre-set, to a flat disk under a closely defined level of force.

The enhanced version of the SHJ proposed by Ramhormozian[9] was called Optimised Sliding Hinge Joint (OSHJ)[10]. The AFCs of the OSHJ are called Optimised Asymmetric Friction Connection (OAFC) in this

paper.

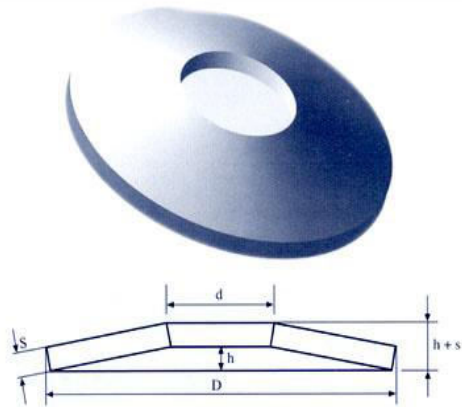


*Fig. 3. A typical Belleville spring design [11]*

The OAFCs bolts, as mentioned before, are tightened in the elastic range and effectively remain elastic during seismic induced sliding, retaining most of their installed bolt tension after significant sliding[10].

## 2 FINITE ELEMENT ANALYSIS

Finite element analysis (FEA) is a very powerful and useful tool for engineering researchers to create a virtual testing programme. The aim of undertaking the FEA study is to simulate, as closely as practicable, the experimental behaviour and then to monitor and analyse important parameters such as forces and stress distribution.

This paper explains creating finite element model (FEM) of the OAFC.

In this study, ABAQUS/CAE v2020/standard software[12], as one of the well-established nonlinear finite element analysis packages, is used for modelling and analysing the samples. The software has the ability to take into account both material and geometrical nonlinearities as well as contact interactions and bolt loads. The procedures for modelling Optimised Asymmetric Friction Connection (OAFC) sample as well as a convergence study on the mesh size and geometry, as well as element type are explained in the following sections.

### 2.1 Modelled specimen

The modelled specimen is based on the experimentally tested components presented in [5, 9]. In this research the focus was on the bottom flange OAFC, as it is shown in the Figure 4.

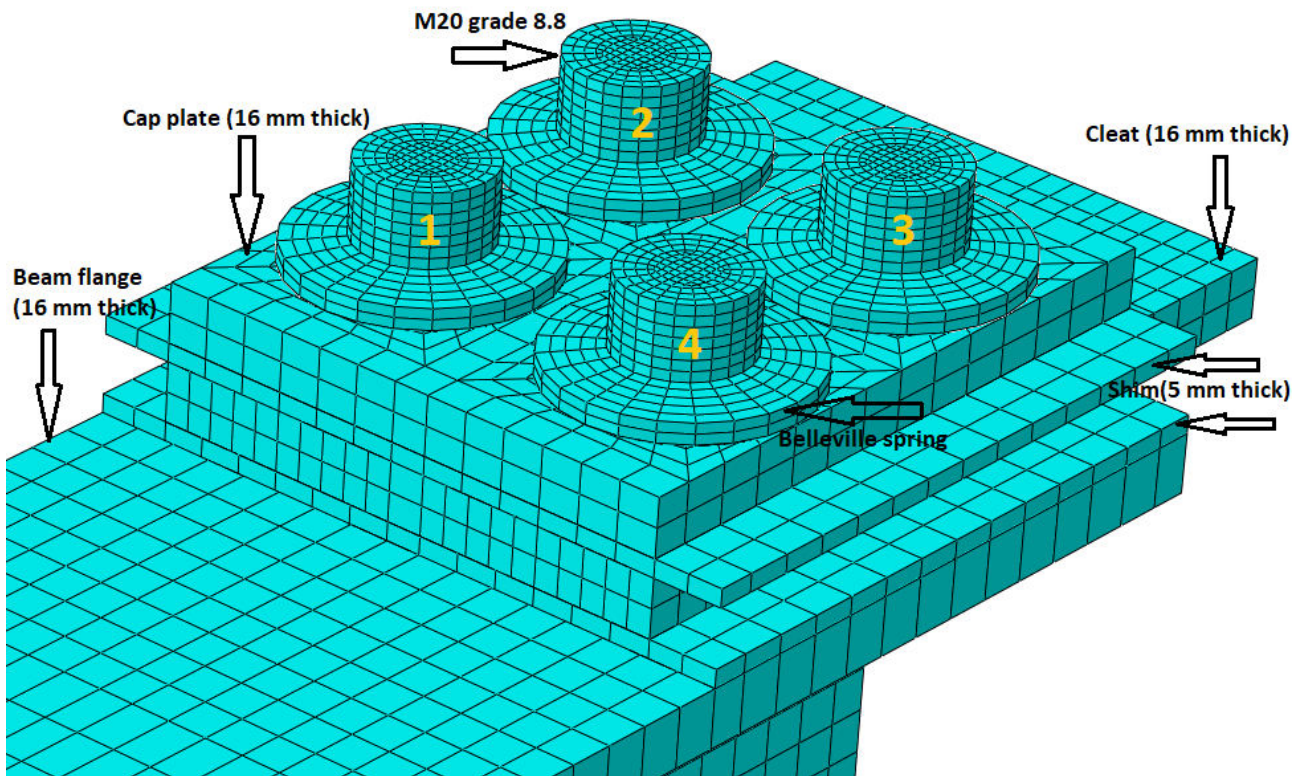


Figure 4: Modelled specimen – Beam Bottom Flange OAFc (Normal mesh).

The bolts are modelled as dumbbell shapes to simplify the model and reduce the computational costs (Fig. 5) for this convergence study. This method has been implemented by other researchers such as [13, 14]. The nut and bolt's head are merged with the bolt body which represents both threaded and unthreaded loaded regions of the shank. The hardened washers are also merged with the bolt head and nut.

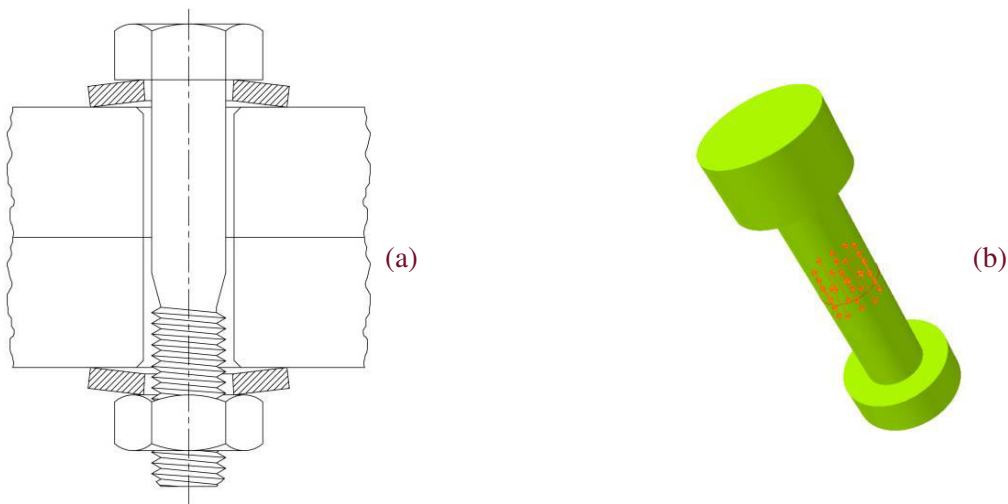


Figure 5: Bolt modelling and applying bolt load. a) Real bolt, b) dumbbell bolt with bolt load.

The installed bolt tension for this analysis is 50% of proof load, which is equal to 106.2 kN considering the dimensions of the bolt and proof load stress of 600MPa [5]. The “bolt load” option is used in ABAQUS software to apply pre-tension in the middle cross section of dumbbell bolts as shown in Fig.5. After applying

the pre-tension to the bolts, their lengths are fixed at their current position. This method is similar to tightening bolts in practice; it also helps to capture the bolt tension changes according to the model's response to the loading regime[15].

## 2.2 Material modelling

The model material characteristics are shown in Table 1. The simplified elastic-perfectly plastic model for the material behaviour is considered.

*Table 1: The FEM components' material properties.*

Component and Material	Density ( $gr/cm^3$ )	Elastic behavior Young Modulus (MPa) Poisson Ratio	Yield Stress (MPa)
Bolt – G8.8	7.85E-009	205000 0.3	660
Shim – Raex450	7.85E-009	205000 0.3	1200
G350 structural Steel (Cap/Cleat/Beam)	7.85E-009	205000 0.3	350
Belleville Spring – AISI 6150 alloy steel	7.85E-009	200000 0.285	415

## 2.3 Contact interaction modelling

Given the importance of friction-sliding nature of the Optimised Asymmetric Friction connection's behaviour, modelling the contact interactions between components correctly is critical to the accuracy of output. A lack of appropriate contact interaction modelling will result in inaccurate results or lead to convergence problems [15]. The number of contact pairs that are defined for simulating OAFc parts is shown in Table 2. The small sliding surface-to-surface discretization method is applied for all the contact pairs. The assigned contact interactions have two types of behaviour: tangential behavior and normal behavior. Coulomb friction is used for tangential contact. Penalty friction formulation is selected for the tangential behavior, and hard contact is chosen for normal behavior [15]. The friction coefficient between the shims and cap, cleat, and the beam is taken as 0.48 according to [9]. The values of the friction coefficient between other contact pairs are taken as 0.2 as proposed by [9]. Moreover, based on definition of master-slave contact algorithm of contact pairs in Abaqus/Standard [12], that nodes on one surface (the slave) cannot penetrate the segments that make up the other surface (the master), as shown in Figure 6, the slave and master surfaces in the model are specified based on their material type in terms of strength and size. In other words, if a larger surface contacts a smaller surface, it would be better to have the larger one as master surface; however, if both surfaces have the same size, the one with the stiffer body (usually the rigid surface) should be the master. The algorithm places no restrictions on the master surface; it can penetrate the slave surface between slave nodes, as shown in Figure 6.

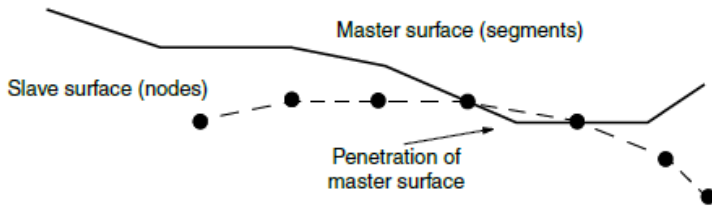


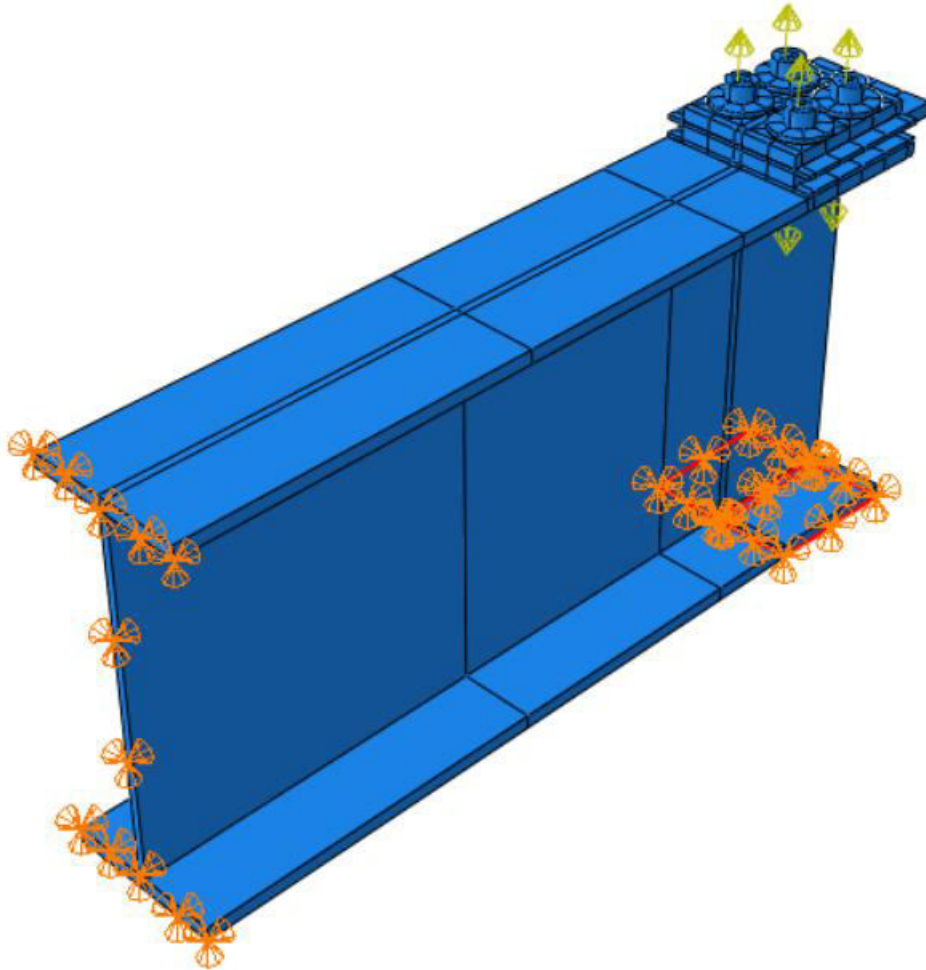
Figure 6: The master surface can penetrate the slave surface.

Table 2: The interaction properties specified in the model. Normal behaviour is hard non penetration contact for all surfaces.

Interactions between (Slaves surfaces - master surfaces)	Interaction properties: Tangential Behaviour; Friction coefficient
Bolts and Cap/Cleat/Beam	0.2
Bolts and Shims	0.2
Shims and Cap/Cleat/Beam	0.48
Belleville Springs and Bolts	0.2
Belleville Springs and Cap/Beam	0.2

## 2.4 Boundary conditions

The beam length has been selected 1000 mm that is more than 4-times longitudinal length of the cleat. This is to provide realistic flexibility around the AFC avoiding a too stiff boundary condition. The model, as shown in Figure 7, represents an upside-down beam, considering the orientations in a real building. Translational displacements in X, Y, and Z directions are prevented at parts of the beam flanges and web, as shown in Figure 7. The horizontal (Z direction) cyclic displacements were applied at the cleat cross section. The reason of including beam in the model was to provide a realistic flexibility and boundary conditions around the OAFC.



*Figure 7: Boundary conditions.*

A cyclic displacement applied on the side of the cleat with three full cycles as figure 8. The maximum displacement in each direction was taken as 14.5 mm associated with a beam-column rotation of 0.030 rad, pushing the OAFC beyond the 2.5% inter-storey drift limit specified by[16].



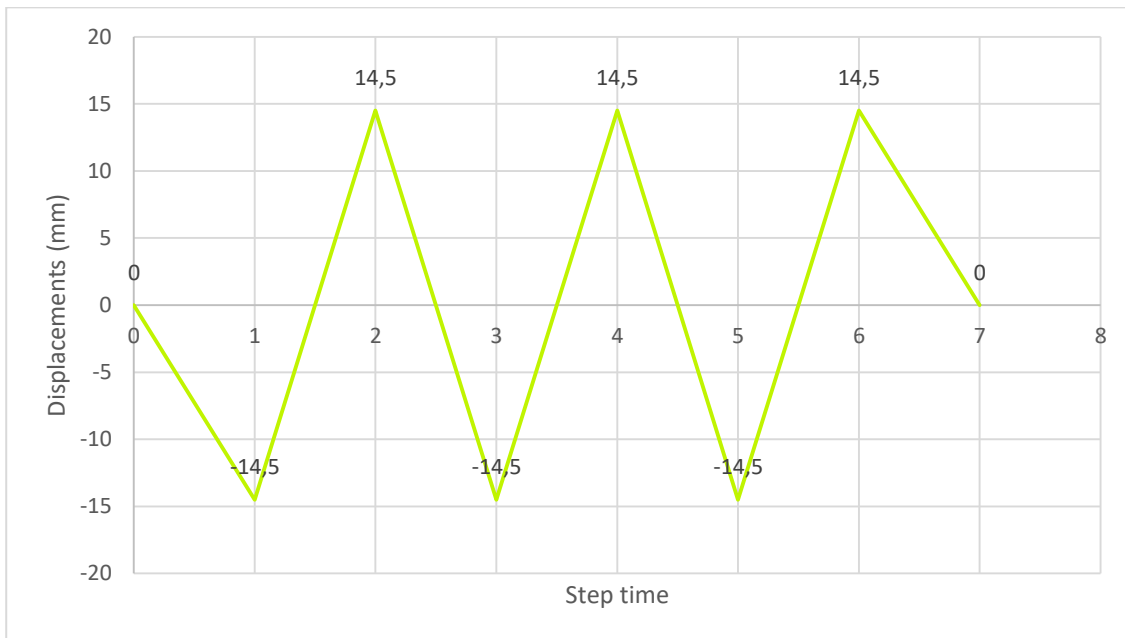
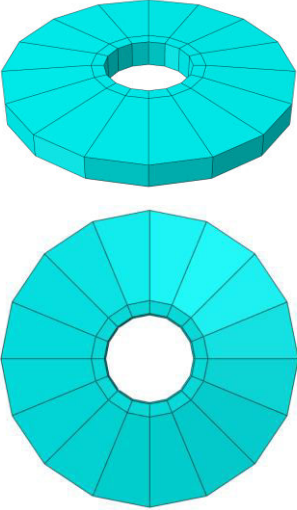
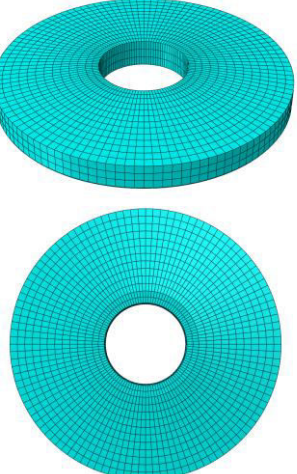
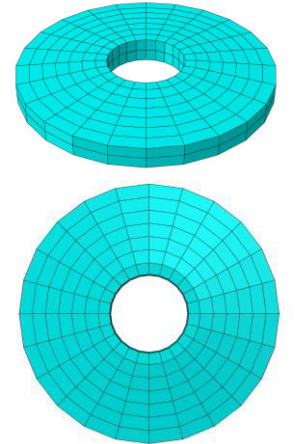
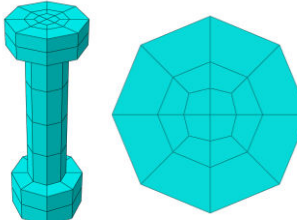
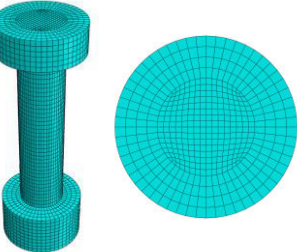
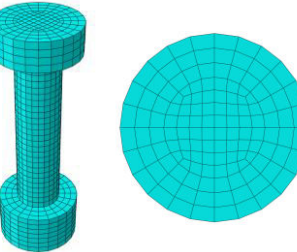
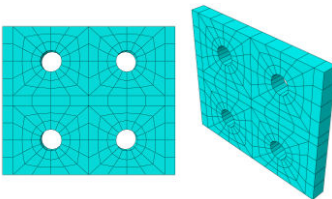
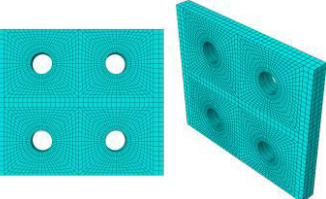
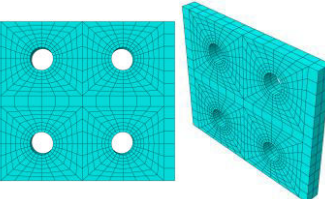
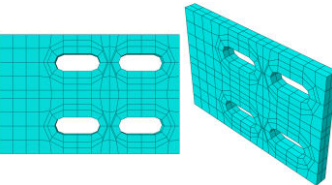
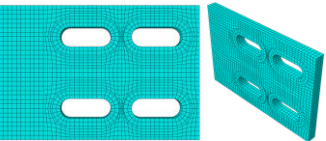
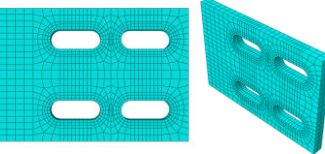


Figure 8: Displacement-based loading regime applied in the Z direction of the cleat edge.

## 2.5 Effect of mesh size on the computational cost and analysis accuracy

Two important influential parameters on the computational cost (time to complete the model analysis) and accuracy of the results are the mesh geometry and size. The structured (mapped) meshing method is implemented to have an appropriate mesh shape (geometry), having smaller size of mesh where the rate of stress and strain changes are expected to be higher. In the modelled OAFC, the high deformation demand is generally on parts namely the bolts, plates, and wall of the holes in contact with the bolts. So, to undertake the convergence (aka sensitivity) study, the mesh size of the bolts, Belleville springs, and the contact area around the holes and through the thickness of the plates (cap, cleat, shims, and beam bottom flange) were considered with three different sizes namely Coarse, Fine, and Normal. Based on this mesh sensitivity study, the “Normal mesh” was considered to be used for the ongoing finite element analysis. The coarse mesh results accuracy was found to be low, while the fine mesh results accuracy was found to be very close to that of the normal mesh. Figure 9 shows the three studied mesh sizes on different components. In the following graphs of bolt tension loss and force versus displacement to compare the effect of the mesh size as well as type of element in the modelling are presented.

Part/Mesh type	Coarse mesh	Fine mesh	Normal mesh
<p data-bbox="172 300 373 331">Belleville Spring</p> <p data-bbox="172 452 373 519">Inner diameter = 20.9 mm</p> <p data-bbox="172 528 373 595">Outer diameter = 69.77 mm</p> <p data-bbox="172 604 373 672">Max Deflection = 1.7 mm</p> <p data-bbox="172 680 373 748">Thickness = 6.35 mm</p>			
<p data-bbox="245 853 303 884">Bolt</p> <p data-bbox="165 925 373 992">Shank diameter = 19.3 mm</p> <p data-bbox="181 1001 373 1068">Shank length = 58 mm</p> <p data-bbox="165 1077 373 1144">Head diameter = 36 mm</p> <p data-bbox="150 1153 395 1220">Thickness = 20 mm top, 12.5 mm bottom</p>			
<p data-bbox="213 1267 325 1299">Cap plate</p> <p data-bbox="172 1352 373 1464">175 mm*150 mm Hole diameter = 22 mm</p>			
<p data-bbox="239 1512 309 1543">Cleat</p> <p data-bbox="165 1637 373 1816">243 mm * 150 mm Hole diameter = 22 mm Hole center- center distance = 35 mm</p>			

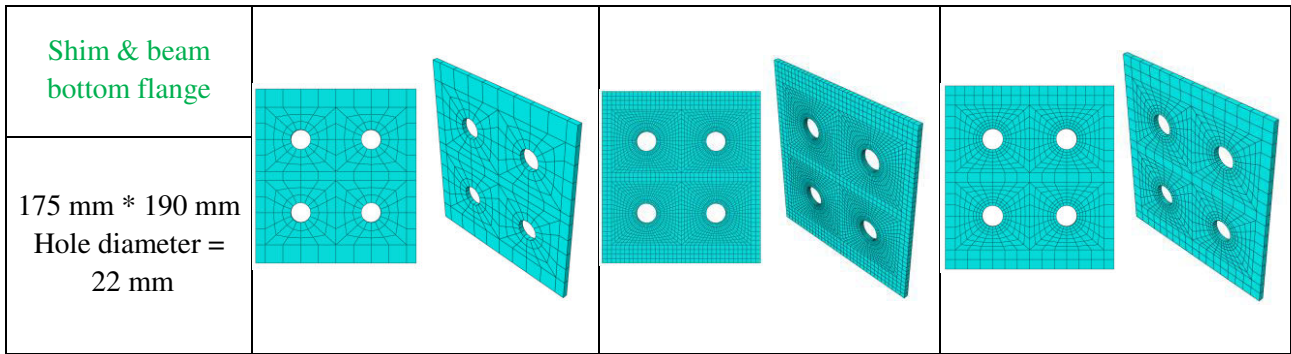


Figure 9: Dimension and different meshes for the contact zone.

Figures 10 to 12 show the reduction of bolt tension for four bolts after sliding in three different models with fine, normal and coarse mesh types, respectively. As shown, 5 steps of analysis are defined, the first step is pre-tensioning and then the displacements are applied up to step 5. All models were in agreement with experimental results [7, 9] in terms of general behaviour suggesting the models were defined adequately. However, the computational cost of running the fine mesh was significant. The analysis time with fine mesh was about three to four times the analysis time with normal mesh. Comparing figures 10 and 11, the model with normal mesh provides a close result to the model with fine mesh. The model with coarse mesh shows inconsistency between different bolts' load history compared with the model with fine mesh.

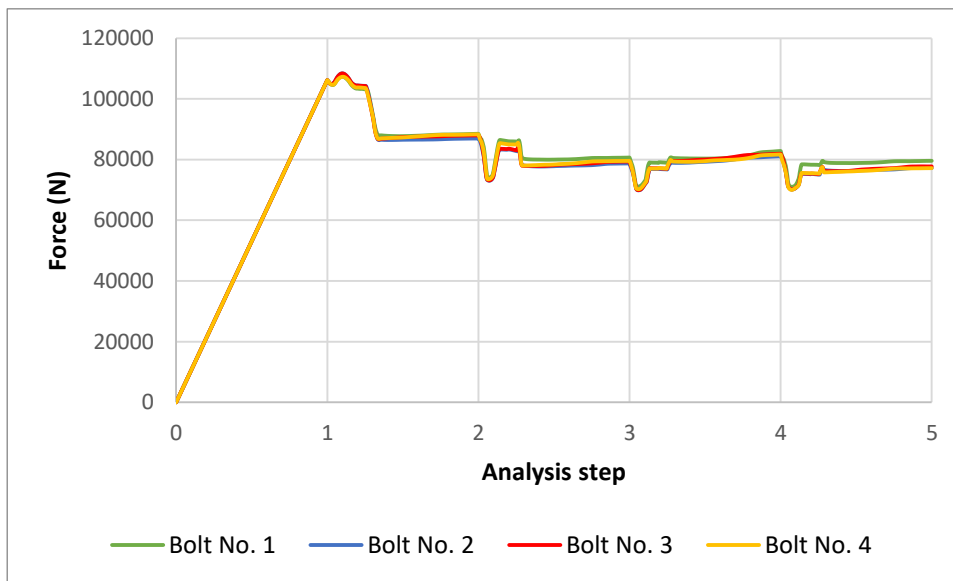


Figure 10: Bolts tension over time with Fine mesh

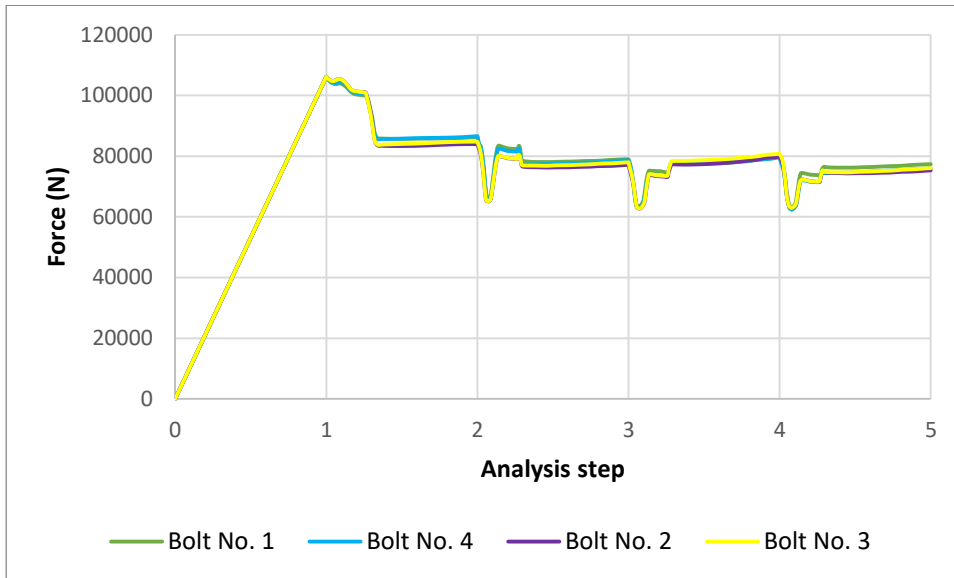


Figure 11: Bolts tension over time with Normal mesh

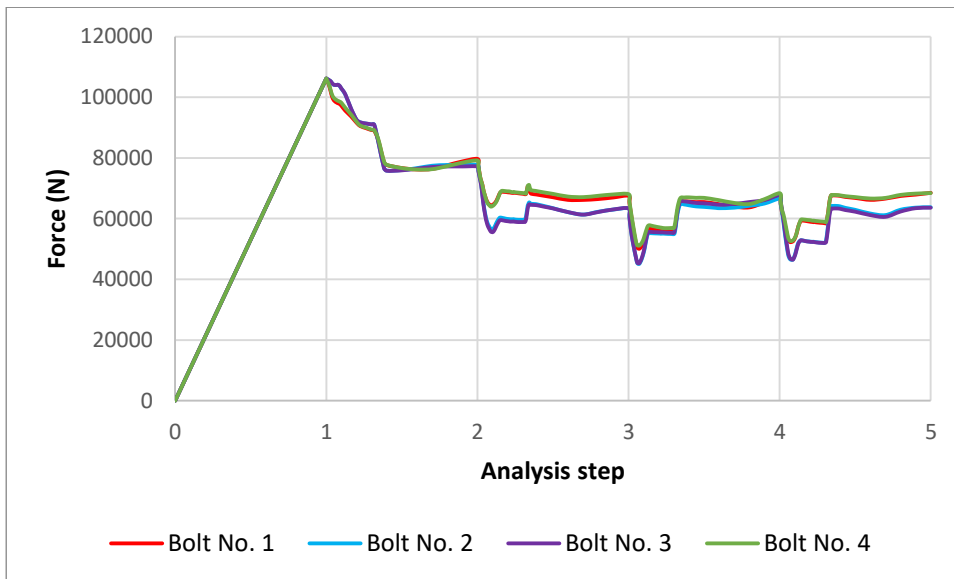


Figure 12: Bolts tension over time with Coarse mesh.

For a better comparison between the three sizes of mesh, Figures 13 and 14 show the bolt tension loss of the third and first bolt, respectively, during sliding with three meshes: fine, normal and coarse. The results of the fine and normal mesh models are very close. This is not the case with the coarse mesh.

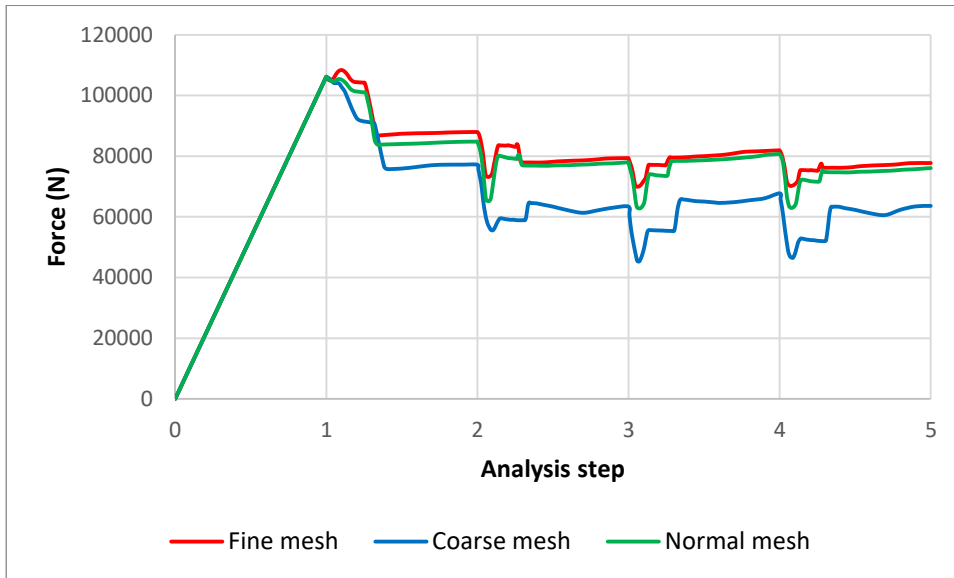


Figure 13: Bolts tension of Bolt No. 3 over time with three sizes of meshes

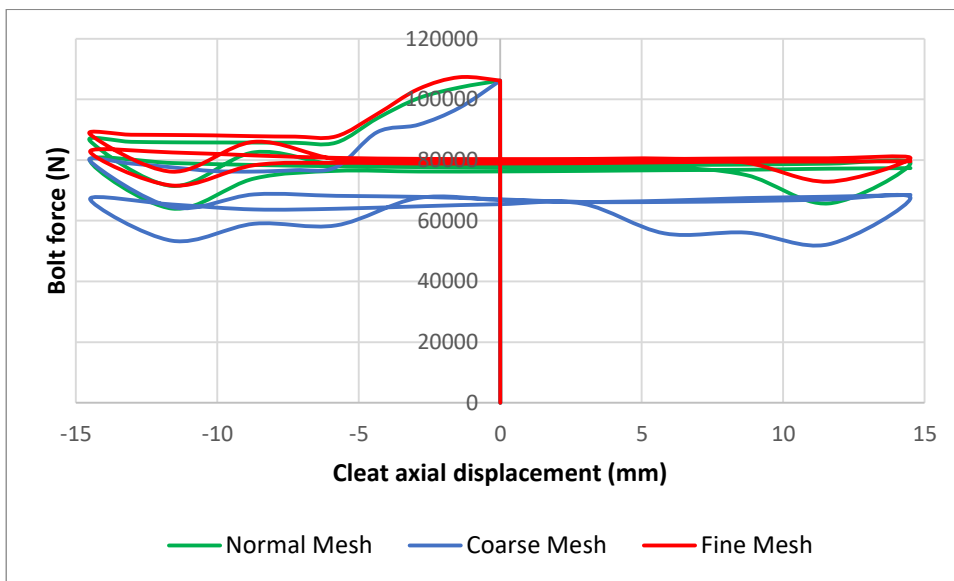


Figure 14: Bolt No. 1 force history for three mesh sizes

Similarly, figure 15 shows that the hysteresis loops of the fine and normal mesh models are very close, and also represent the expected behaviour according to the experimental results [7]. While the coarse mesh models' hysteresis loop shape is as expected, it underestimate the friction sliding force compared with the fine and normal mesh models.

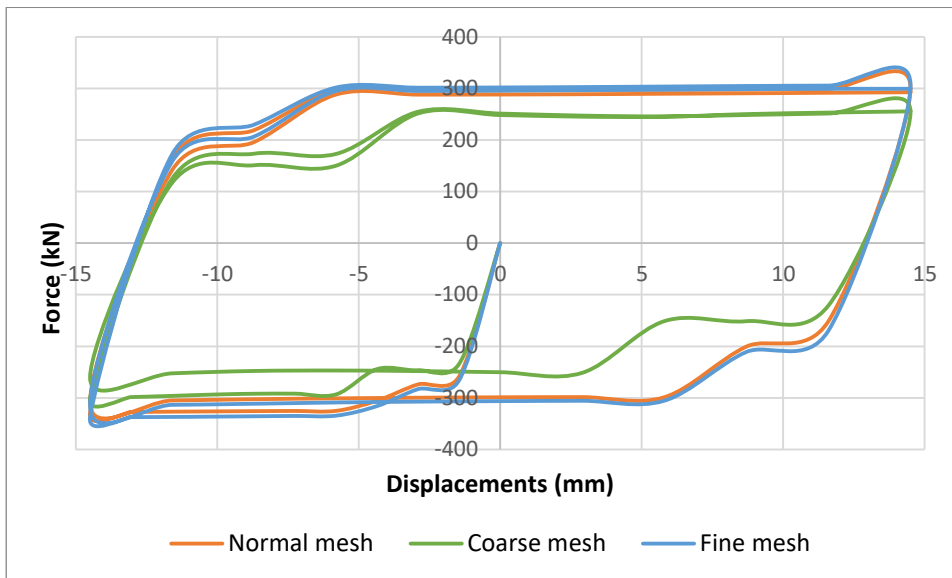


Figure 15: Forces vs displacements applied on the end of the cleat (i.e. hysteresis loop).

## 2.6 Element types

The typical meshed Optimised Asymmetric Friction Connection, which is investigated in this study, is shown in Fig. 4. Within Abaqus[15], there are two available orders of interpolation, namely linear and quadratic. In linear interpolation order, the elements have nodes only at their corners, while in Quadratic interpolation, the elements have corner nodes and mid-side nodes. The Formulation of an element dictates the underlying mathematical algorithms governing element behavior. Fundamentally, there are two distinct types of elemental behavior: Lagrangian and Eulerian. The Lagrangian model describes elements which deform with the material, whereas Eulerian elements are fixed in space and allow material to flow through them[12, 15]. For obvious reasons, this means that Lagrangian elements are appropriate for stress/displacement analyses and Eulerian elements are typically more suitable for representing fluid mechanics [12]. So, in this study, two types of Lagrangian elements including C3D8R and C3D8I were investigated and the beam bottom flange, bottom flange plate (cleat), cap plate, two shims at both sides of the cleat, Belleville Springs, and the pre tensioned high strength friction grip (HSFG) structural bolts are simulated by the eight node linear brick elements with reduced integration (C3D8R element type), and also fully integrated (C3D8I element type). Each node of these elements has three translational degrees of freedom. The analysis using C3D8R element type was completed while the analysis using C3D8I element type was aborted before completion. The comparison of the result between the two elements is presented in Figures 16 and 17.

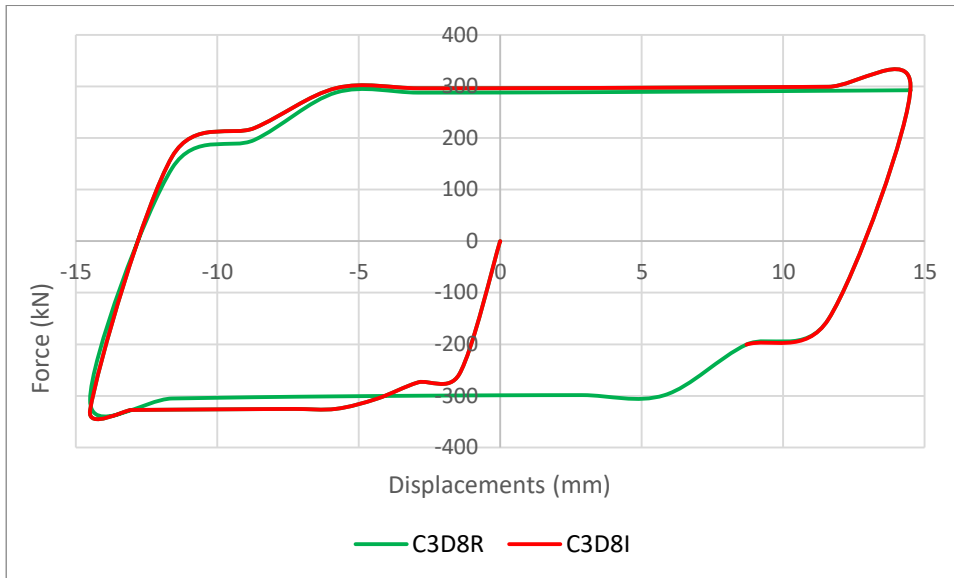


Figure 16: Forces vs displacements applied on the end of the cleat

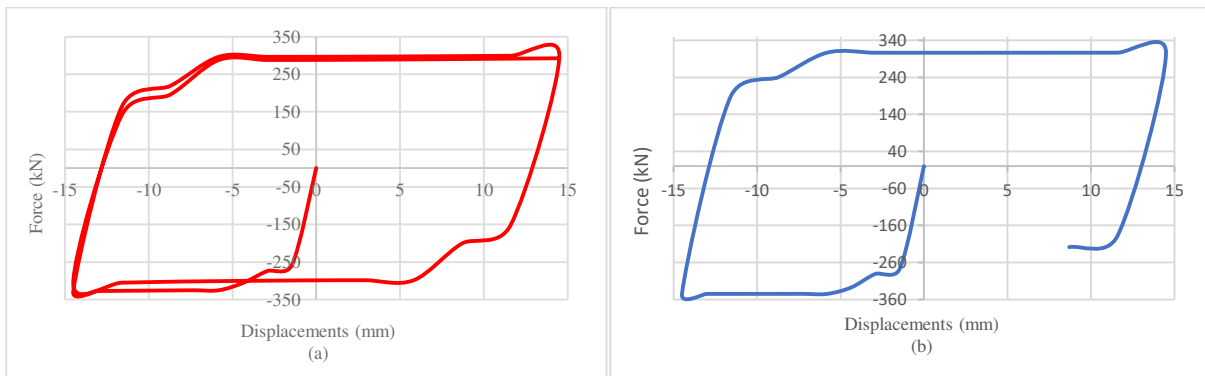


Figure 17: Forces vs displacements applied on the end of the cleat – (a) C3D8R element, (b) C3D8I element

### 3 CONCLUSIONS

Finite-element analysis is an efficient and cost-effective tool to complement experimental investigations of engineering systems. However, creating accurate models to simulate realistic behaviour of the systems requires following appropriate approach for modelling and analysis. This is to avoid facing convergence, accuracy, and computational cost issues. This paper has explored the use of ABAQUS software to numerically analyse the behaviour of Asymmetric Friction Connection, to optimize the size and geometry of the mesh as well as elements type. A cyclic displacement-based loading regime, including three full cycles, were applied on the connection. According to the convergence study undertaken on three different mesh sizes and two different elements, it was found that the results were generally not very sensitive to the mesh size unless extremely coarse meshes were used, hence the optimum mesh size was proposed. Moreover, as selecting the appropriate element type with respect to the simulation objectives is necessary to obtain accurate results, two potentially ideal elements were used. The C3D8R element type was found to be the appropriate element for this study. The numerical results were presented suggesting the models are in good agreement with experimental results [7, 9] in terms of general behaviour.

## 4 ACKNOWLEDGEMENT

The support from New Zealand Ministry of Business, Innovation and Employment (MBIE) through an Endeavour Fund for the Research Programme (Sustainable Earthquake Resilient Buildings for a Better Future - PROP-83779-ENDRP-AUT) is greatly appreciated.

## 5 REFERENCES

1. Pall, A. *Performance-based design using pall friction dampers-an economical design solution*. in *13th World Conference on Earthquake Engineering, Vancouver, BC, Canada*. 2004.
2. Hamburger, R.O. and K. Frank. *Performance of Welded Steel Moment Connection: Issues Related to Materials and Mechanical Properties*. in *Steel Seismic Issues Workshop, Session*. 1994.
3. Engelhardt, M.D. *Ductile detailing of steel moment frames: basic concepts, recent developments and unresolved issues*. in *Proceedings, XIII Mexican Conference on Earthquake Engineering*. 2001.
4. MacRae, G., C. Clifton, and S. Innovations. *Low damage design of steel structures*. in *Steel Innovations 2013 Workshop, Christchurch, New Zealand*. 2013.
5. Ramhormozian, S., G.C. Clifton, G.A. MacRae, G.P. Davet, and H.-H. Khoo, *Experimental studies on Belleville springs use in the sliding hinge joint connection*. *Journal of Constructional Steel Research*, 2019. **159**: p. 81-94.
6. Ramhormozian, S., G.C. Clifton, G.A. MacRae, and G.P. Davet, *Stiffness-based approach for Belleville springs use in friction sliding structural connections*. *Journal of Constructional Steel Research*, 2017. **138**: p. 340-356.
7. Clifton, G.C., *Semi-rigid joints for moment-resisting steel framed seismic-resisting systems*. 2005, University of Auckland.
8. Khoo, H., *Development of the low damage self-centering Sliding Hinge Joint*. 2013, University of Auckland.
9. Ramhormozian, S., *Enhancement of the sliding hinge joint connection with belleville springs*. 2018, University of Auckland.
10. Ramhormozian, S. and G.C. Clifton, *Optimised Sliding Hinge Joint (OSHJ): Design and Installation Guide for a Low Damage Seismic Resisting System*. 2020: New Zealand Heavy Engineering Research Association.
11. Ramhormozian, S., G. Clifton, and G. MacRae, *The asymmetric friction connection with belleville springs in the sliding hinge joint*. NZSEE, Auckland, New Zealand, 2014.
12. Systèmes, D., *ABAQUS 6.14 Getting Started with Abaqus: Interactive Edition*, in *ABAQUS 6.14 Getting Started*. 2014.
13. Ramhormozian, S., G.C. Clifton, Y. Cui, M. Poirot, A. Ashikov, and G.A. MacRae. *Finite Element Analysis (FEA) of the Asymmetric Friction Connection (AFC) with and without Belleville Springs (BeSs) in the Sliding Hinge Joint (SHJ) Connection*. in *12th Pacific Structural Steel Conference (PSSC'19) Tokyo, Japan*. 2019.
14. Mago, N., *Finite element analysis of the sliding hinge joint R.-.* 2002, Editor. 2002, HERA.
15. Systèmes, D., *Abaqus analysis user's guide*. Solid (Continuum) Elements, 2014. **6**: p. 2019.
16. Zealand, S.N., *NZS 1170.5: 2004, Structural design actions part 5: earthquake actions-New Zealand*. Standards New Zealand, Wellington, 2004.